coatings

MDPI

Article

Heat-Seal Ability and Fold Cracking Resistance of Kaolin-Filled Styrene-Butadiene-Based Aqueous Dispersions for Paper-Based Packaging

Andrea Marinelli [1,2,*], Mauro Profaizer [3], Maria Vittoria Diamanti [1,2,*], MariaPia Pedeferri [1,2] and Barbara Del Curto [1,2]

[1] Department of Chemistry, Materials and Chemical Engineering "Giulio Natta", Politecnico di Milano, Piazza Leonardo Da Vinci 32, 20133 Milan, Italy
[2] National Interuniversity Consortium of Materials Science and Technology (INSTM), Via Giuseppe Giusti 9, 50121 Firenze, Italy
[3] Ghelfi Ondulati, Via dei Lavoratori 10, 23010 Buglio in Monte, Italy
* Correspondence: andrea.marinelli@polimi.it (A.M.); mariavittoria.diamanti@polimi.it (M.V.D.); Tel.: +39-02-2399-3137 (M.V.D.)

Abstract: Dispersion coatings are offered as alternative solutions to extrusion coating technology for paper-based packaging. In addition to providing barrier properties, waterborne dispersions may implement the processing and converting properties of coated substrates, which are of extreme interest for an effective transfer to the industry. In this work, styrene-butadiene-based aqueous dispersions were formulated considering different amounts of kaolin as pigment. The authors assessed the heat-seal ability, fold cracking resistance, and blocking tendency, comparing the results against commercial dispersion coating grades. Kaolin content dominated the sealing behavior of experimental formulations, changing the minimum heat-seal temperature from 80 °C to >140 °C for 0% and 60% kaolin solid content, respectively. On the contrary, commercial grades were mostly affected by temperature. Additionally, despite the low latex glass temperature (0 °C), experimental formulations generally showed little, if any, blocking. On the downside, increasing kaolin content eases fold cracking, showing a different magnitude according to fold direction and coat orientation yet achieving a higher moisture barrier compared to commercial grades for both folded and unfolded samples.

Keywords: coated paper; clay; aqueous dispersion; mechanical properties; fold cracking

Citation: Marinelli, A.; Profaizer, M.; Diamanti, M.V.; Pedeferri, M.; Del Curto, B. Heat-Seal Ability and Fold Cracking Resistance of Kaolin-Filled Styrene-Butadiene-Based Aqueous Dispersions for Paper-Based Packaging. *Coatings* **2023**, *13*, 975. https://doi.org/10.3390/coatings13060975

Academic Editors: Giorgos Skordaris and Frederic Debeaufort

Received: 9 March 2023
Revised: 7 May 2023
Accepted: 22 May 2023
Published: 23 May 2023

1. Introduction

Paper-based packaging is currently in the spotlight and widely considered a sustainable alternative to polymeric packaging. Embracing the material transition, the paper industry was required to coat cellulosic substrates to improve their durability and barrier properties. Among the ways to surface coat paper and board, aqueous dispersions represent a rapidly growing technology that is gaining much more interest from the industry and market [1].

Aqueous dispersion coatings are polymeric water-based colloidal dispersions of polymeric particles, involving possible further substances, e.g., mineral pigments and fillers, dispersants, defoamers, and thickeners [2,3]. Among some of their positive traits, dispersion coatings make it easier to achieve thinner coating thickness compared to other technologies, e.g., extrusion coating. Consequently, aqueous dispersions can reduce the non-cellulosic content of packaging, possibly improving the final recyclability [4–6]. Nevertheless, aqueous dispersions are generally more expensive than conventional coating

technologies. To cope with coating price, pigments can be added, which may also improve barrier properties [7–13] to, e.g., liquids, gases, and oil and grease.

Not only can pigments provide barrier properties, but they can also affect the converting process. Indeed, pigment content influences printability, gluing ability, heat-seal ability, and many more [8,9]. Considering coated paper reels and sheets, it may be interesting to investigate heat-seal ability and fold cracking resistance.

Heat-seal ability involves one layer sealing to another surface due to the combined effects of pressure and temperature over a defined seal time. Such a property is of high interest at an industrial level to produce sealed packaging, e.g., pouches, lidded trays, and pillow bags; this is well documented in the recent literature [14–17]. Proper and uniform sealing is a crucial condition for preventing issues such as accidental packaging opening and content spills while guaranteeing packaging barrier performance.

Another interesting yet important processing property is blocking, which is defined as the tendency of a possible adhesive surface to adhere to another surface, regardless of whether it is potentially adhesive or not. Similar to heat sealing, blocking behavior can be driven by the combined effects of time, temperature, and pressure [18]. When developing a coated material, it is crucial to ensure that during storage and transportation of the semi-finished products, the materials do not stick together. Otherwise, it may become very difficult—if not impossible—to unwind the reel or, equivalently, feed the machine at the converting plant. Previous literature discussed the effect of increasing the pigment ratio inside aqueous dispersions on both blocking and heat-sealing, showing how it is desirable for blocking yet unfavorable for heat-sealing ability [8,9,17].

When processed, substrates in the form of sheets typically need to be folded as part of the process to convert them into finished packaging. Such processing is widely reported to generate cracks, especially in the coating layer; many studies have provided numerical models to describe and predict fold cracking of coated paper [19–24]. Coat cracking, however, affects both the aesthetic and functional properties, letting water, grease, and moisture permeate through the packaging material. This in turn may reduce the shelf-life of packed goods, which may be essential to prevent issues such as food loss; this is of major interest even when the impact of food is greater than that of packaging [25].

Therefore, it is crucial for packaging producers, material developers, and researchers to also test converting properties instead of barrier ones alone. In this way, a thorough characterization may be achieved, widening the fields of application for the aqueous dispersions as well as identifying possible issues to be overcome prior to the scale-up process. Embracing this perspective, this work aims to provide a propaedeutic discussion of the effects and magnitude of the technological parameters that affect the processing of dispersion coatings, introducing a comparison between current commercial formulations and alternatives of possible industrial relevance that can be produced in a laboratory.

In this contribution, the authors investigated the effect of different kaolin contents in polymeric aqueous dispersions with respect to the above-mentioned converting properties of coated paper substrates, searching for statistically evident factor significance. The research assessed the heat-seal ability, blocking tendency, and fold cracking of flexible cellulosic packaging; furthermore, the results were compared to commercially available heat-sealable grades.

2. Materials and Methods

2.1. Substrate

In this work, Mondi (Weybridge, UK) ProVantage Komiwhite (125 g/m^2, 0.155 mm thick) virgin kraft fiber substrate was considered. The substrate is a white top kraft liner and is commonly used in cellulose-based packaging production. Due to its low grammage, it can be used both in flexible and rigid packaging (in the latter situation as a layer, e.g., in corrugated cardboard).

2.2. Commercial Coatings and Experimental Coatings Formulation

HPH 39 highly crosslinked carboxylated styrene-butadiene latex (dry solid content 54%) was kindly provided by Trinseo (Horgen, Switzerland). Amberger Kaolinwerke (Hirschau, Germany) CamCoat 80 kaolin (aspect ratio = 28) was used as the pigment in the experimental formulations; 62% of the particles possess a size that is less than 2 μm. Kaolin Critical Pigment Volume Concentration (CPVC) was measured using spatula rub-out linseed oil absorption.

Coating preparation followed the procedure described in a previous publication [7]. EXOlat C40 sodium polyacrylate, used as dispersant (0.16% dry on dry pigment), was kindly provided by PCC Exol SA (Brzeg Dolny, Poland). A target of 50% solid content was set for the experimental formulations. Sodium hydroxide was added to adjust the pH to 8.

Four different formulations were produced, as reported in Table 1.

Table 1. Experimental coating formulations for HPH 39 styrene-butadiene latex.

Abbreviation [1]	Latex	Filler	Latex:Filler Ratio [%]
H39K 100	HPH 39	Kaolin	100:0
H39K 80	HPH 39	Kaolin	80:20
H39K 60	HPH 39	Kaolin	60:40
H39K 40	HPH 39	Kaolin	40:60

[1] H39 stands for HPH 39, whereas K stands for kaolin.

The properties analyzed and discussed in this manuscript were compared to those of three heat-sealable commercial aqueous dispersions. The nomenclature corresponds with a previous study [7] (nature of the latex and possible pigment, followed by "H", to highlight that it is a commercial heat-sealable coating):

- SA-H: styrene acrylate dispersion coating with a dry solid content of 50% (on a weight basis)
- A-H: acrylate copolymer dispersion coating with a dry solid content of 39% (on a weight basis)
- SAP-H: styrene acrylate dispersion coating filled with 6% of pigment with a dry solid content of 51% (both percentages are on a weight basis)

No modification or addition was made to the aqueous dispersions, which were used as provided.

Before their application on the cellulosic substrate, both commercial and experimental aqueous dispersions were stirred with a magnetic anchor for at least 30 min at 500 rpm.

2.3. Differential Scanning Calorimetry

All waterborne dispersions were analyzed with Differential Scanning Calorimetry (DSC) to obtain the characteristic glass transition temperature. A DSC3 Mettler Toledo (Columbus, OH, USA) was used to test the samples in a nitrogen atmosphere (flow 60 mL/min). Then, a ramp of 20 °C/min was set in a −30–300 °C temperature range. The analysis involved oven-dried samples with a weight of 10–20 mg placed in a 40 μL aluminum pan.

2.4. Sample Preparation

The paper was manually rod-coated using a 12 μm (wet film thickness) K-Bar number 2 at a constant speed of 40 mm/s on the white side. Immediately after coating application, the substrates were fixed in open-ended frames and dried in an oven at 120 °C for 90 s to let heat act on both sides of the paper. Subsequently, a cool down step to ambient

conditions occurred. Following this, the samples were cut out of the coated paper—according to the specific dimensions for each test—and conditioned at 23 °C and 50% relative humidity for >24 h.

Reference values were measured from uncoated (UC) samples.

The dry coat thickness of the experimental formulations was calculated from the composition of the formulations, considering a latex density of $\varrho = 1.05$ g/cm^3 and a kaolin density of $\varrho = 2.6$ g/cm^3 [7].

2.5. Barrier Properties

Commercial coating grades underwent barrier properties testing to test possible improvements in the water barrier as well as moisture and grease permeability properties. All the tests were carried out at standard temperature and humidity conditions (23 °C and 50% relative humidity, respectively), considering triplicate samples for each coating and test.

Water barrier property was measured by means of the Cobb 1800 test as per BS EN ISO 535:2014 [26]. The test evaluates the water absorption tendency of the coated substrate under 10 mm deep water for 30 min. The standard defines water absorptiveness as:

$$\text{Water Absorptiveness (Cobb1800)} = \frac{m_1 - m_0}{A} \quad (1)$$

where m_1 is the final sample mass (in grams), m_0 is the initial mass (in grams), and A is the test area (in m^2). The test area was limited to almost 40 cm^2 due to the reduced sample dimensions.

Moisture permeability was assessed via the Water Vapor Transmission Rate (WVTR) gravimetric method, following the procedure described in BS ISO 2528:2017 [27]. WVTR cups were filled with 35.0 ± 0.1 g of silica gel, and the test lasted 48–96 h, depending on the barrier performance of the specific coated sample. The samples were positioned with the coated side facing the inner side of the cup. The test area of the samples was approximately 20 cm^2. WVTR was determined by evaluating the steady slope of the cup mass gain in time, as described in Equation (2):

$$\text{WVTR} = \frac{24 \cdot \alpha}{A} \quad (2)$$

where α is the steady slope (in g/h), A is the test area (in m^2), and 24 is the factor to achieve WVTR in g/(m^2·day). Finally, grease permeability was measured in accordance with BS ISO 16532-1:2008 [28]. In the test, palm kernel oil is spread on the sample and a fixed mass weight is applied to the upper surface for a maximum of 24 h. The test measures the time that the coated substrate resists grease permeation through coated paper, and stain formation is observed on the back of the samples. Higher recorded times highlight higher grease resistance.

2.6. Heat-Seal Ability

The ability to seal (coat-to-coat) was assessed considering the effect of three different parameters that can be easily controlled during the sealing process: temperature, time, and pressure. The value ranges for the variables are reported in Table 2.

Table 2. Investigation matrix for the heat-seal ability.

Parameter	Unit	Values
Temperature	°C	80, 100, 120, 140
Time	s	1, 2
Pressure	MPa	0.4, 0.6

All the coatings were tested under at least two out of four temperature conditions. In the results, data are reported starting from the lowest temperature at which it was possible

to achieve minimum adhesion between the coated surfaces. Three 80 mm × 15 mm paper strip pairs were coat-to-coat sealed and tensile tested for each combination, for a total of 48 samples for each aqueous dispersion. Samples were sealed using a flat tool over a square area of 15 mm × 15 mm. Heat-sealing was carried out using an ad-hoc machine developed by the authors, which is driven by Arduino and involves a pneumatic circuit that acts on a pneumatic cylinder. Further information is reported in Appendix A.

Average seal strength and seal energy were obtained from tensile tests using a Shimadzu (Kyoto, Japan) Autograph AGS-X mounted on a 5 kN load cell. In this study, the test speed was set to 100 mm/s. Each tail was secured in opposing grips, leaving the seal unsupported during the test.

2.7. Blocking

Coated substrates underwent blocking tendency as per BS EN 12702-2000 [29] to 40 °C, 60 °C, and 80 °C. The test was conducted in triplicate for each coating and test temperature. In this study, the thermoplastic blocking of a potential adhesive surface (the coated one) was assessed against the back of the KB substrate. This allowed us to evaluate the blocking tendency of a coated reel when stocked.

2.8. Fold Cracking

The resistance to cracking upon folding was assessed both according to the folding direction (parallel to the machine direction or orthogonal to it) and to the coating orientation (facing inside or outside the fold).

The test involved 10 mm-wide strips that were subjected to a 180°-fold under 1 kg weight, like in a recent study [30]. However, the fold time was reduced to 1 s compared to the work of Breskvar et al. [30]. The limited time was set to be closer to industrial times. The weight was then removed, and the strip was carefully opened flat. Following this, a cotton swab soaked in Pelikan Tusche A vermilion-red drawing ink was rapidly passed on the folding line, taking care to immediately wipe excess ink with absorbent paper. In doing this, if cracks were present, the ink could find a way through the coating to reach the fibers underneath, which in turn would absorb it and macroscopically highlight the coating discontinuities.

For each condition and coating, 12 samples were folded, and pictures were acquired at constant magnification (120×). Finally, the images were processed with ImageJ v1.53e to measure the stained area (in pixels) over a length of 5.5 mm for each sample.

Additionally, the authors assessed the WVTR of folded samples (under 1 kg for 1 s) to assess the effect of possible fold cracking on the moisture barrier properties. The fold was carried out according to the worst condition observed in the fold cracking test (coating outside and fold orthogonal to the machine direction).

2.9. Statistical Analysis

Statistical analysis was performed using Minitab 21.3.1. Linear Pareto charts represent the analysis of the experimental response surface design regression. Pareto charts aimed to assess the relevance of processing parameters during heat-sealing for both experimental and commercial aqueous dispersions. Coating (for commercial grades) and latex content (for experimental formulations) factors were set at categorical factors to assess the effect of the same nominal processing factors, i.e., temperature, time, and pressure.

Analysis of variance (ANOVA) and Tukey pairwise analysis were conducted to highlight statistical differences among experimental formulations in terms of equivalent fold cracking area.

Standard deviation is reported in the figures as error bars, whereas tables report such value in parenthesis.

2.10. Scanning Electron Microscope (SEM)

Samples were analyzed using a ZEISS EVO 50 (Zeiss, Wetzlar, Germany) scanning electron microscope (SEM). SEM micrographs were mainly used to assess the coating morphology to look for possible fold cracking and voids in the cross section of kaolin-filled aqueous dispersions.

3. Results

3.1. Sample Preparation

The coated samples tested in this work achieved an overall average dry coat grammage of 7.9 ± 2.4 g/m^2. Table 3 shows the actual dry coat grammages and thicknesses for each formulation. The authors report no issues encountered during the application and drying of the aqueous dispersions. Grammage variation was mainly attributed to the manual application of the coatings; lower solid content contributed to achieving below-average grammages for the A-H samples.

Table 3. Dry coat grammages and coat thicknesses. Standard deviation is indicated in parenthesis.

Coating	Dry Coat Grammage [g/m^2]	Coat Thickness [μm]
H39K 100	9.2 (1.6)	8.9 (1.5)
H39K 80	8.0 (1.3)	5.9 (1.0)
H39K 60	7.7 (2.0)	4.6 (1.2)
H39K 40	9.1 (1.5)	4.6 (0.8)
SA-H	7.5 (2.6)	7.2 (2.5)
A-H	4.7 (1.5)	4.5 (1.6)
SAP-H	9.2 (2.0)	8.8 (2.0)

The theoretical critical pigment volume concentration for kaolin is reported to be around 60% [11]. Given its density, 60% kaolin content by weight leads to almost 38% volume concentration. The spatula rub-out test resulted in 41% CPVC, similarly to a previous work [31]. Since the pigment volume concentration (PVC) was close to the CPVC just determined, the authors needed to assess void absence in the coatings. Samples cross sections were then SEM analyzed. A representative SEM micrograph of a H39K 40 cross section is visible in Figure 1, showing no visible void in both the coat cross-section and coat surface, hence PVC < CPVC.

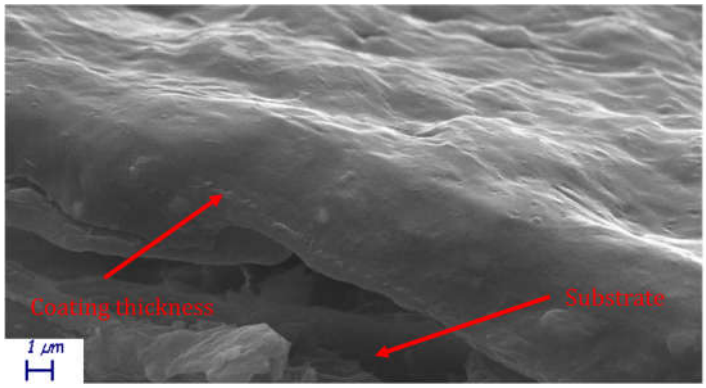

Figure 1. H39K 40 coating cross-section SEM micrograph.

3.2. Differential Scanning Calorimetry

DSC results are reported in Table 4. The data show how almost every grade involved in the experimentation is characterized by two glass transition temperatures. This highlights the multiphase polymeric nature of the formulations.

Interestingly, kaolin content affects the measured T_g, requiring higher temperatures for higher pigment content. Such an increase, however, is limited to 5 °C for a 60% weight increase in kaolin content compared to the unpigmented latex. At the highest kaolin concentrations, however, the noise produced by the pigment made the second T_g undetectable.

Table 4. Glass temperature of the different coating formulations and grades involved in this study.

Coating	T_{g_1} [°C]	T_{g_2} [°C]
H39K 100	−0.6	19.0
H39K 80	0.9	35.3
H39K 60	2.8	33.3
H39K 40	4.6	
SA-H	−6.1	39.1
A-H	47.1	75.2
SAP-H	12.1	

3.3. Barrier Properties

All the assessed barrier properties are reported in Figure 2. Please note that results were normalized to a coat thickness of 7 µm, following the procedure described by Marinelli et al. [7]. This is due to the crucial role of coat thickness, which increases and reduces coat defects and provides higher performance.

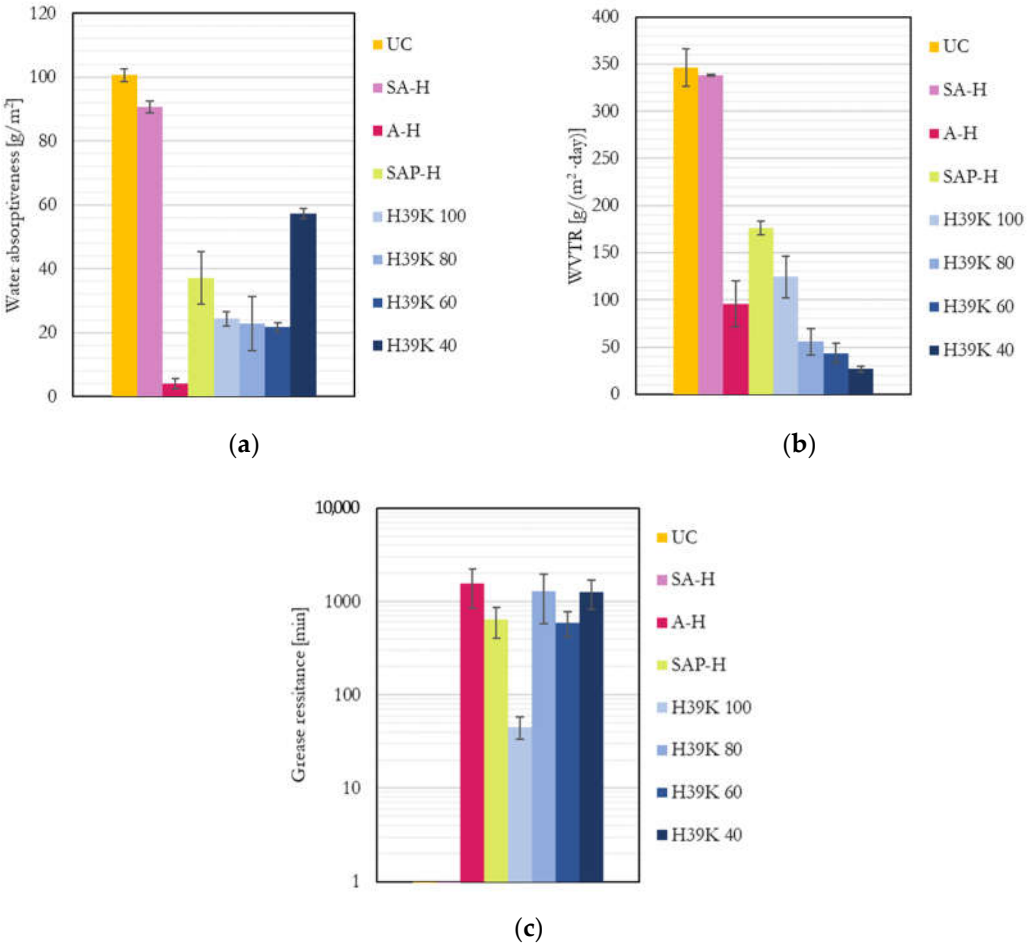

Figure 2. Barrier properties for the uncoated (UC), commercial (SA-H, A-H, and SAP-H), and experimental dispersion coatings: (**a**) Water absorptiveness; (**b**) Water vapor transmission rate; (**c**)

Grease permeability (UC and SA-H are not visible since they resist <1 min). The values for the experimental formulations were taken from Marinelli et al. [7].

As clearly visible, compared to the experimental formulations, the properties of commercial grades varied significantly, showing almost no performance to all the barriers in the case of SA-H (indeed, it performed as UC); similar water and grease barrier properties (but worse than moisture) in the case of SAP-H; and a higher water yet similar moisture and grease barrier in the case of A-H. Unsurprisingly, the experimental coatings generally underperform commercial barrier grades [7], yet they provide competitive barrier properties, as shown in some other studies in the literature [13]. Kaolin allows higher performance against water vapor diffusion due to the increased tortuous path required for the molecules to pass through the coating; the WVTR decreased as pigment content increased, as expected. However, such behavior could not be found in previous research [32], probably due to the absence of bubbles in the coating even at higher kaolin ratios, as shown in Figure 1. Most importantly, kaolin allows a marked improvement in grease resistance with respect to pure latex formulations due to its hydrophilic surfaces [7]. A statistically significant correlation was found for WVTR and grease permeability (correlation = −0.732; $p = 0.007$) for experimental formulations at different kaolin contents. The negative correlation factor suggests that kaolin plays a crucial role in increasing the permeation times (reducing transportation rates) of both moisture and grease and increases pigment content.

Compared to experimental pigment-filled dispersions, SAP-H generally provided lower performance despite the reduced amount of pigment, highlighting how the latex may play a crucial role in determining the overall properties.

3.4. Heat-Seal Ability

In general, three main curves can be obtained during the peel test (Figure 3), representing three main behaviors, respectively:

- Absence of or negligible heat-seal ability, characterized by average force < 1 N (Figure 3a);
- Adhesive separation occurring at the coat–coat interface, characterized by an almost linear curve in which the average force ranged 1–2.5 N (Figure 3b); a possible alternative curve was characterized by a sequence of peaks representing inhomogeneous adhesion throughout the sealed area, attributed to too little time to allow an even interdiffusion of the polymeric fraction of the coats (Figure 3c);
- Cohesive failure of the substrate, highlighting a seal and coat-substrate interfacial bond, stronger than the one keeping the paper fibers together. In general, such behavior occurred at average forces > 2.5–3 N, which corresponds with previous literature [16] (Figure 3d). The curve is characterized by a peak force, beyond which the substrate fails and substrate delamination occurs [33].

The processed results, i.e., seal energy and average force, are reported in Table 5 and Figures 4 and 5.

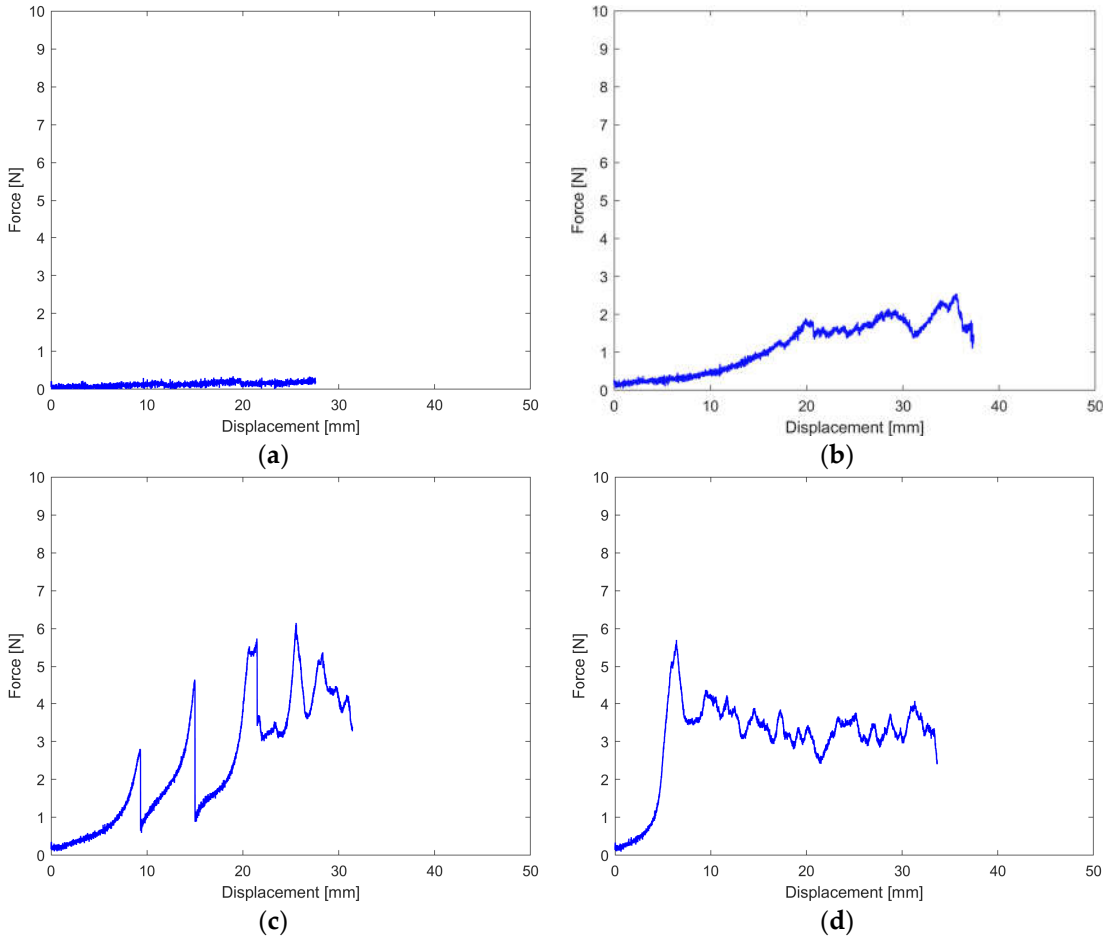

Figure 3. Typical Force-Displacement tensile test curves of the heat-sealed samples: (**a**) Negligible seal; (**b**) Adhesive separation of the sealed sample, occurring at the coat-coat interface; (**c**) Inhomogeneous seal, with peaks highlighting decently sealed areas; (**d**) Cohesive failure of the substrate, substrate delamination.

Table 5. Mean Heat-Seal energy and standard deviation (indicated in parenthesis) measured for the tensile-tested samples.

Heat-Seal Energy [mJ]																	
Coat	***T [°C]***	***80***				***100***				***120***				***140***			
	t [s]	***1***		***2***		***1***		***2***		***1***		***2***		***1***		***2***	
	P [MPa]	***0.4***	***0.6***	***0.4***	***0.6***	***0.4***	***0.6***	***0.4***	***0.6***	***0.4***	***0.6***	***0.4***	***0.6***	***0.4***	***0.6***	***0.4***	***0.6***
H39K 100		94 (31)	108 (20)	111 (6)	107 (18)	116 (3)	98 (5)	99 (4)	114 (5)	103 (14)	98 (7)	113 (13)	103 (6)	-	-	-	-
H39K 80		29 (20)	44 (22)	110 (14)	109 (20)	119 (5)	113 (20)	113 (3)	113 (10)	101 (6)	90 (9)	88 (3)	112 (2)	-	-	-	-
H39K 60		-	-	-	-	16 (10)	25 (10)	35 (10)	81 (17)	8 (6)	20 (20)	102 (20)	107 (8)	111 (11)	103 (16)	115 (6)	113 (12)
H39K 40		-	-	-	-	-	-	-	-	-	<1	<1	<1	2 (1)	<1	2 (2)	3 (1)
SA-H		1 (1)	1 (1)	41 (30)	8 (8)	100 (28)	104 (6)	98 (10)	109 (17)	132 (7)	123 (17)	101 (22)	105 (17)	-	-	-	-
A-H		-	-	-	-	<1	<1	2 (1)	3 (2)	9 (3)	11 (1)	84 (15)	92 (8)	74 (4)	96 (12)	108 (19)	83 (5)
SAP-H		<1	1 (1)	3 (2)	11 (5)	3 (2)	5 (1)	54 (35)	46 (12)	108 (21)	112 (7)	121 (3)	117 (10)	-	-	-	-

The effect of increasing kaolin content in the experimental formulations is clearly visible. As shown in Figure 4a, which presents the minimum tested pressure and time, H39K 100 is fully sealed at 80 °C, whereas H39K 40 cannot seal even at 140 °C. Instead, H39K 80 requires at least 100 °C, and H39K 60 requires 140 °C.

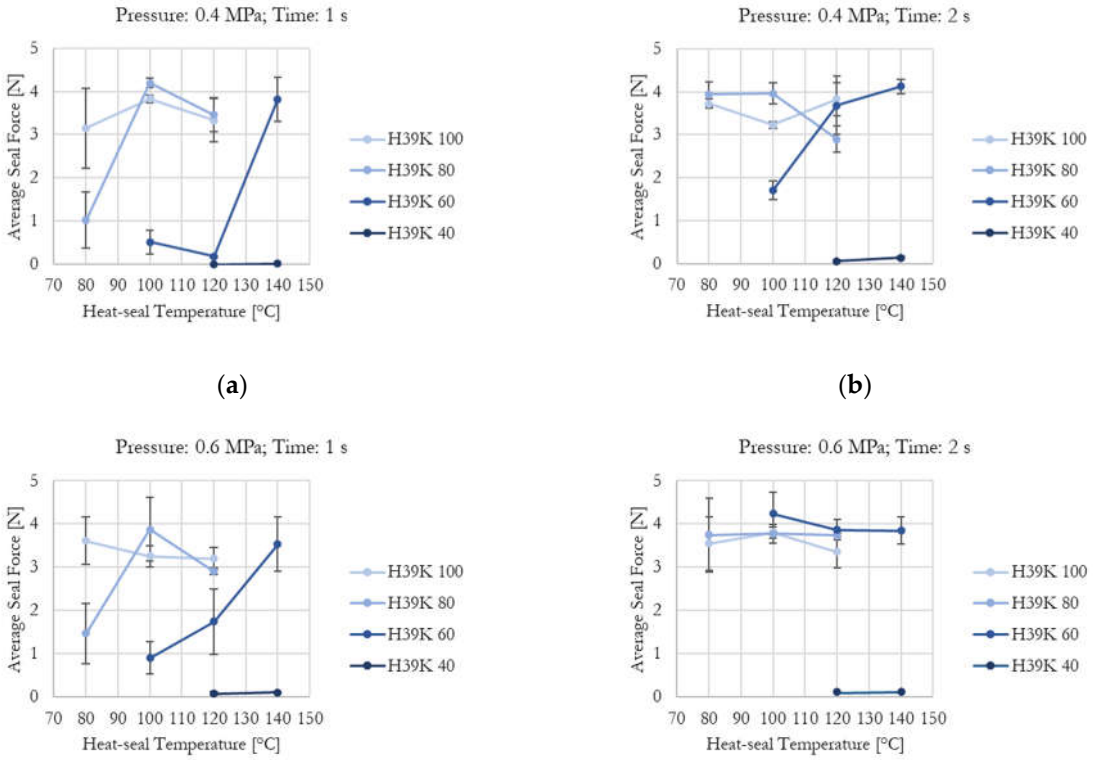

Figure 4. Kaolin content, temperature, time, and pressure effect on average seal force for experimental formulation-coated samples: (**a**) Pressure = 0.4 MPa, time = 1 s; (**b**) Pressure = 0.4 MPa, time = 2 s; (**c**) Pressure = 0.6 MPa, time = 1 s; (**d**) Pressure = 0.6 MPa, time = 2 s. Higher kaolin content requires higher values for the investigated parameters to improve sample seal-ability.

In principle, temperature is a crucial factor since it influences chain mobility. Yet, actual coat temperature also depends on time, which highly influenced both commercial and experimental grades under constant temperature–pressure seal conditions (Figures 4 and 5). Indeed, the temperature–time graph represents a transient curve that depends on the nature of the material to be heated, and on its thickness. Therefore, higher seal times allow, in principle, a more homogeneous temperature distribution across the sealed area, but with temperatures that are closer to the ones set for the seal tools. The seal pressure effect seemed residual (Table 5).

The effect of the factor was assessed by a linear Pareto chart for both experimental and commercial coatings and for both average seal force and seal energy. The results are reported in Figure 6. Interestingly, the factors that are statistically significant differ between experimental formulations and market-available dispersions. The latex content plays a major role in the development of formulations, followed by time and temperature, respectively. Their effect, however, is quite limited compared to the one that kaolin content has. This explains the crucial role of kaolin platelets in reducing the sealing promotion of the coatings. The seal temperature range to achieve cohesive behavior is, however, consistent with commercially coated papers [34], showing how even 20% pigment content is adequate to ensure the interdiffusion ability of the polymeric latex film. For higher kaolin contents, the fine dimension of the particles may act like contaminant agents in the

polymeric layers [35], reducing the seal integrity. Additionally, given the low thermal conductivity of kaolin [36], higher pigment fractions explain the longer processing times required to guarantee proper polymer interdiffusion in combination with the reduced latex volume.

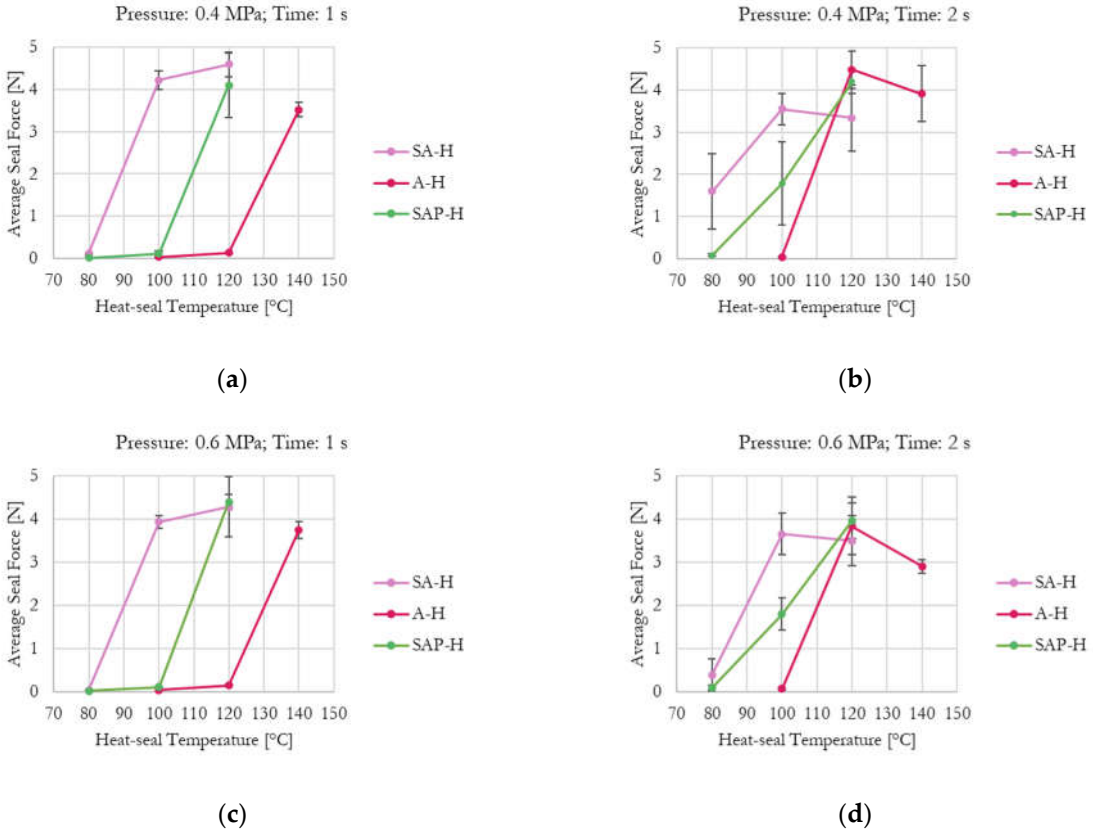

Figure 5. Effect of the investigated parameters (i.e., temperature, time, and pressure) on average seal force for commercial grade-coated samples: (**a**) Pressure = 0.4 MPa, time = 1 s; (**b**) Pressure = 0.4 MPa, time = 2 s; (**c**) Pressure = 0.6 MPa, time = 1 s; (**d**) Pressure = 0.6 MPa, time = 2 s.

Commercial grades, due to having little or no pigment, are mostly affected by the temperature set during the heat-sealing process, followed by the specifically considered grade, i.e., latex nature and chain mobility. Time seems to be statistically relevant only for seal energy. A similar computation of different data on multilayer films [37] (standardized effect: time = 8.798; temperature = 7.940; reference value = 2.026) coherently agrees on the leading effect of time.

For both coating groups, pressure played a residual role, highlighting how the pressure difference may be too low to significantly affect the investigated properties. Such a result is consistent with previous research [15]. Seal pressure might, however, become an essential factor to optimize when creased substrates need to be sealed, avoiding any leaks [38].

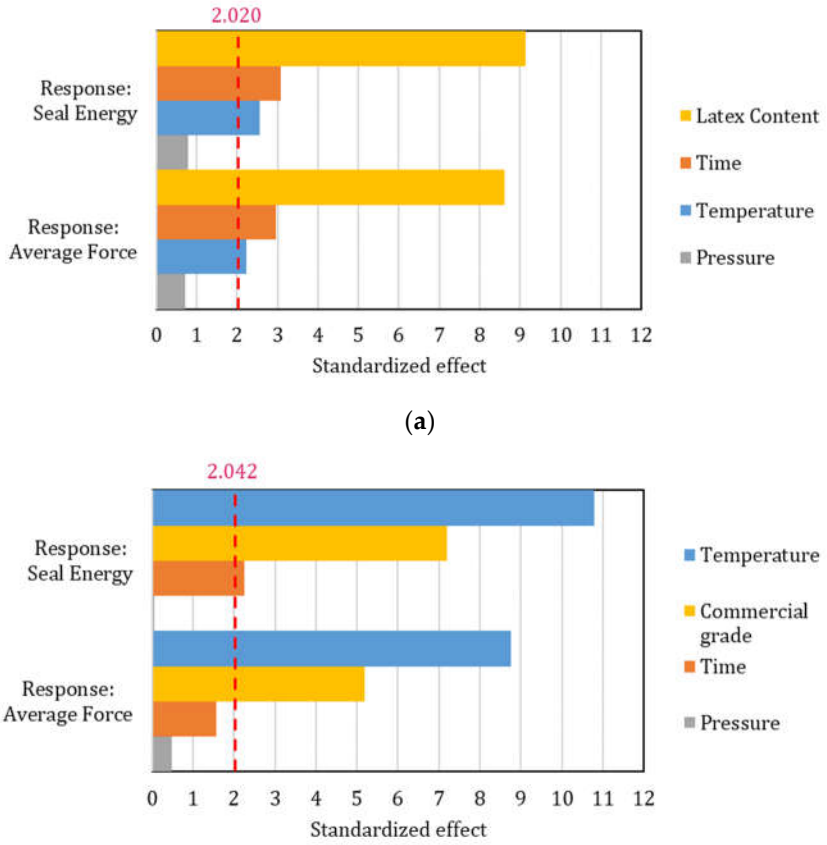

Figure 6. Linear Pareto chart for the standardized effect of the considered factors. Both seal energy and average force responses are reported in each graph: (**a**) Experimental formulations; (**b**) Commercial grades. The dashed line represents the reference line above which the effect of the factors is statistically significant.

3.5. Blocking

Samples generally showed little, if any, blocking tendency (Table 6). First-degree blocking occurred for H39K 100 at 40 °C, which means adhesion without fiber detachment from the substrate in contact with the coating. The other coatings rarely showed traces of first-degree blocking, which, due to their negligible extent, were classified as coatings that did not block. Such behavior highlighted the reduced blocking tendency of coatings containing increasing inorganic pigment content, as also reported in previous literature [9,11].

Table 6. Blocking level for the different commercial and experimental aqueous dispersions investigated.

	Blocking Level		
Coating	**40 °C**	**60 °C**	**80 °C**
SA-H	0 *	0 *	0 *
A-H	0	0	0 *
SAP-H	0 *	0 *	0 *
H39K 100	1	1	1
H39K 80	0 *	0 *	0 *
H39K 60	0	0	0
H39K 40	0	0	0

* Negligible traces of blocking were detected.

3.6. Fold Cracking

The equivalent area (in mm²) of the ink-highlighted cracks is reported in Figure 7. In general, no or only small marks were found in folded samples with the coating on the inside. Additionally, the crack area is higher when the fold is orthogonal to the machine direction (MD) (parallel to the cross direction, CD), which is consistent with previous studies [20,30,39]. This can be explained by the anisotropy of the substrate, which has fiber orientation that influences the area subjected to stresses, which should be, in turn, proportional to the overall crack area [39]. Additionally, such anisotropy is reflected in the mechanical properties of the substrate. Excluding SA-H, looking at the outside orientation of the coating as it is for the retrieved literature involving fold cracking, a fold parallel to MD produces a cracked area that is up to 60% lower compared to the same fold but orthogonal to MD. Lower reduction percentages were achieved for highly-filled experimental formulations (H39K 40 and H39K 60) due to the increased coating brittleness, i.e., due to lower binder content, as also observed in highly-filled coatings [40]. This is confirmed by the trendline of the experimental formulations, which is similar for every fold cracking test condition reported in Figure 7.

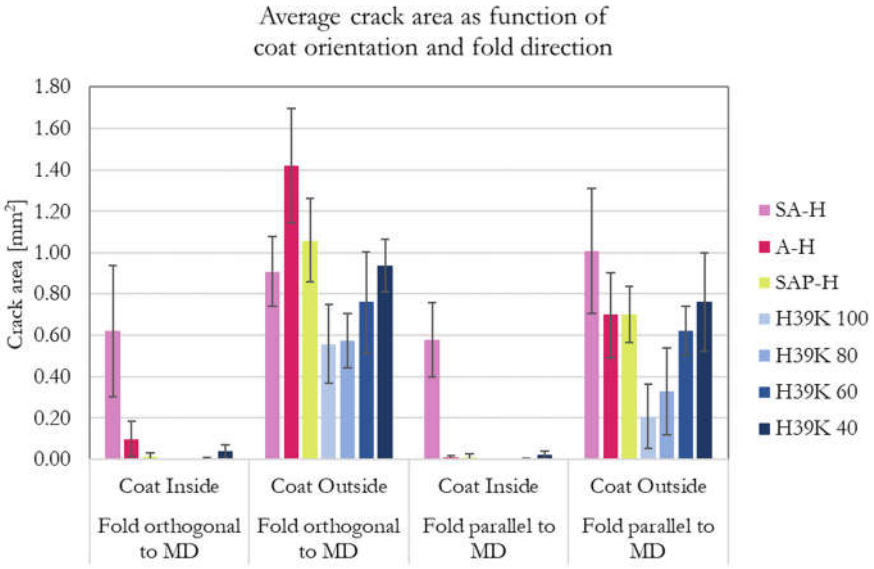

Figure 7. Equivalent fold cracking area (in mm²) for the different coating. The histogram shows the effect of coat orientation (inside or outside the fold) and fold direction (parallel, or orthogonal to MD). Bars that are not visible represent zero crack areas.

ANOVA statistical analysis was performed for the experimental formulations with a confidence level of $\alpha = 0.05$. Each group (folding set of conditions) provided a p-value of $p = 0.000$, highlighting statistical evidence for different means for different pigment content. Additionally, Tukey pairwise comparison was performed (95% confidence level) and the results are reported in Table 7. Regardless of coat orientation, both folding directions highlighted a statistical difference for H39K 40, highlighting that kaolin content should be kept well below 60% (dry weight basis). Interestingly, the Tukey method called attention to the behavior of the outside coating orientation. While folding orthogonal to MD requires a 40% difference in pigment content, folding parallel to MD highlighted a statistical difference when pigment content increased from 20% to 40% (dry weight basis).

Table 7. Tukey method grouping information (95% confidence).

Coating	Folding Set of Conditions			
	Orth. to MD Coat Inside	Orth. to MD Coat Outside	Par. to MD Coat Inside	Par. to MD Coat Outside
H39K 40	A	A	A	A
H39K 60	B	A, B	B	A
H39K 80	B	B, C	B	B
H39K 100	B	C	B	B

Representative pictures are reported in Figure 8. Specifically, all coatings behaved similarly to H39K 60 (left column), except for SA-H, which was more difficult to analyze. Indeed, due to the almost null water barrier, the coating absorbed the ink, making it harder to select the red area due to reduced saturation differences.

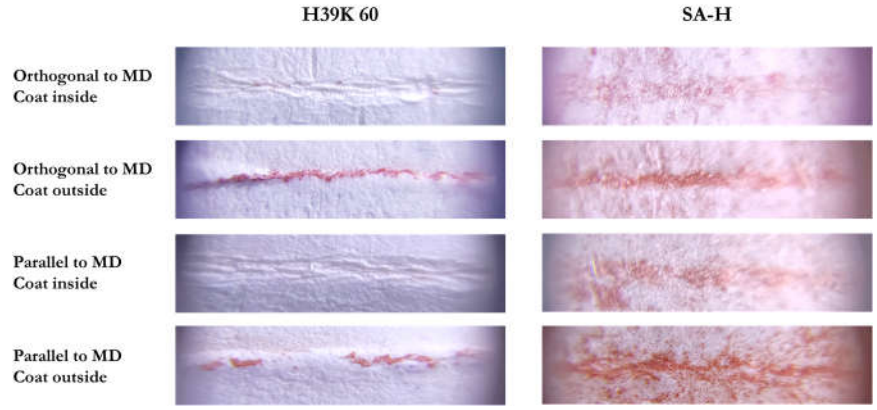

Figure 8. Representative images that were analyzed with ImageJ. The left column is representative not only for H39K 60, but also for the other coatings. On the contrary, SA-H was the only one showing a different behavior.

Representative SEM micrographs of the fold cracked areas are reported in Figures 9 and 10, showing the worst folding condition (coating facing outside, fold direction orthogonal to MD) according to different kaolin content and commercial coatings and different coat orientation and fold direction for H39K 80, respectively. In general, the cracks presented in Figure 9 show a continuous crack without secondary cracks, even at higher magnifications. This behavior is different compared to that highlighted in [41], and this is mainly attributed to the reduced coat grammage. Indeed, the outer surface of thicker coatings is subjected to higher tensile stresses, which imply a higher tendency for secondary crack formation in highly filled formulations.

Additionally, the clearly visible fibers (Figure 9) highlight how possible delamination occurred in the paper substrate, further facilitating the water vapor transportation rate at the crack surface.

When the coating was faced towards the inside during the folding procedure, a larger deformation area could be seen, as shown in Figures 10a,b. However, no crack was found, showing that compressive stresses were distributed over a wider area.

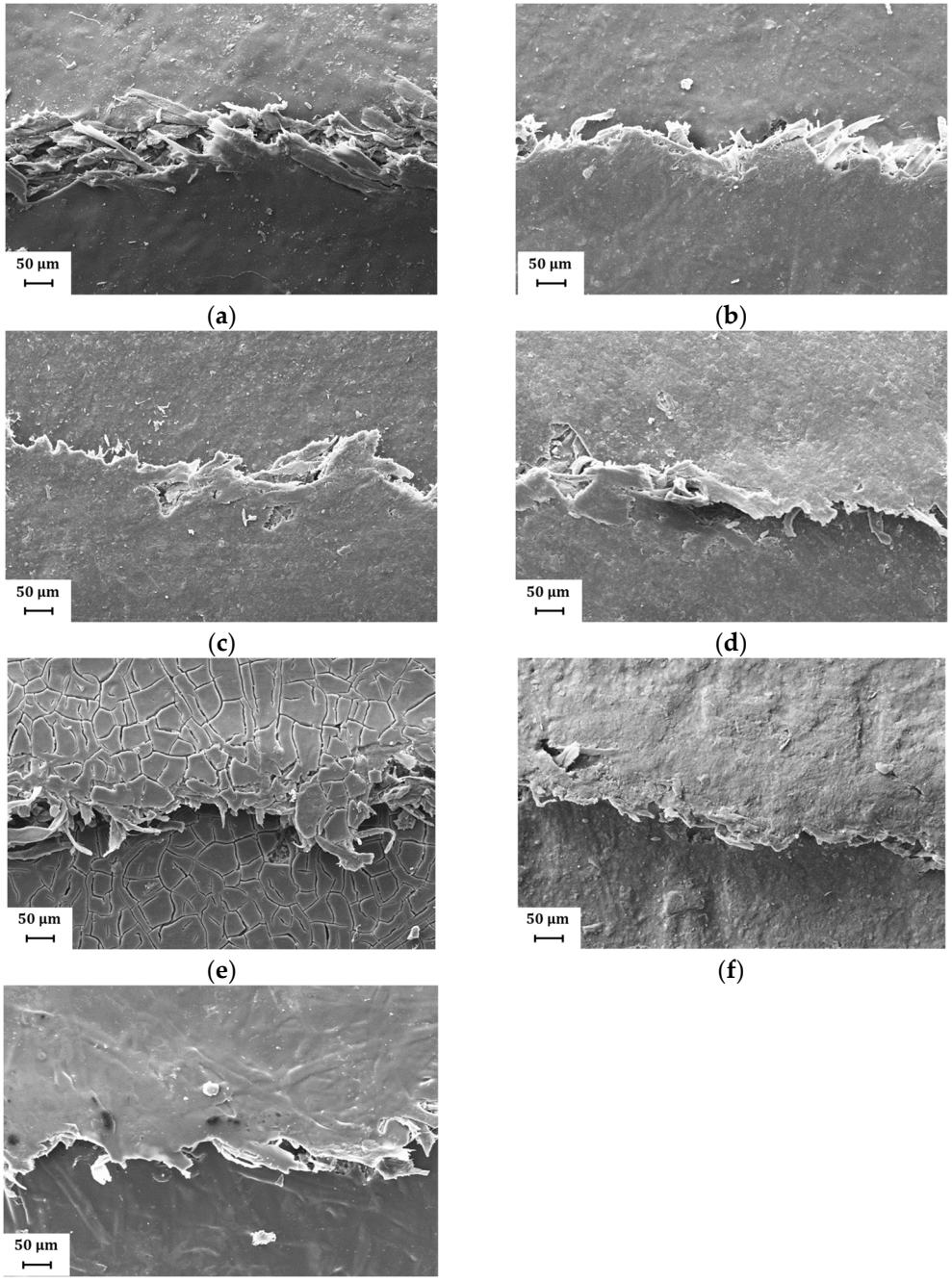

Figure 9. Representative SEM images (magnification: 500×) showing the fold crack at different kaolin content and commercial coatings: (**a**) H39K 100; (**b**) H39K 80; (**c**) H39K 60; (**d**) H39K 40; (**e**) SA-H; (**f**) SAP-H; (**g**) A-H.

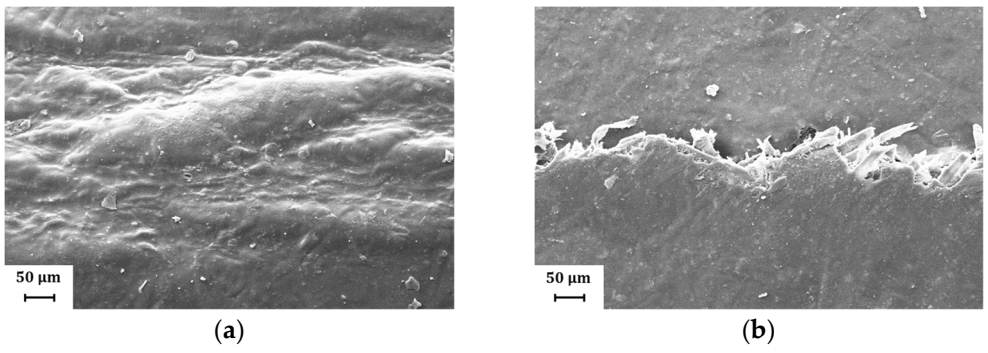

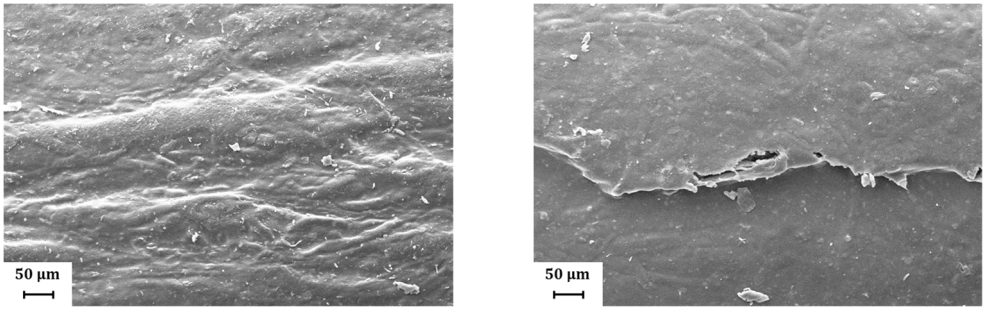

(**c**) (**d**)

Figure 10. Representative SEM images (magnification: 500×) showing the fold crack morphology for H39K 80: (**a**) Coat inside, fold orthogonal to MD; (**b**) Coat outside, fold orthogonal to MD; (**c**) Coat inside, fold parallel to MD; (**d**) Coat outside, fold parallel to MD. Cracks are present only for the sets involving the coat side facing outside during the folding.

The effect of folding on WVTR led to an increased moisture transmission rate. The extent of such an increase was different for each coating (Figure 11), depending on the original barriers. Indeed, the lower the unfolded WVTR, the higher the effect of fold cracks, showing a Pearson correlation of −0.793 (p = 0.000). The highest increase was obtained for H39K 40, which doubled in value, whereas SA-H, due to the cracked surface (Figure 9e), showed little variation. The Pearson correlation factor between the unfolded and folded samples was 0.998 (p = 0.000). Such results highlight how, in line with the equivalent fold cracking area (Figure 7), each sample was affected by crack formation. Thus, avoiding defects in the processing of the material is crucial.

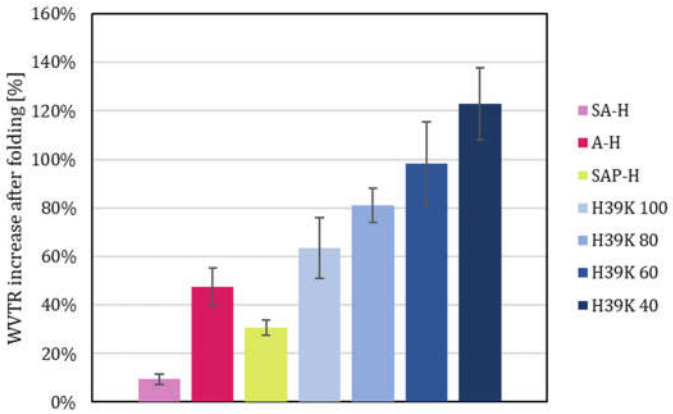

Figure 11. WVTR relative increase for each coated sample due to folding.

4. Discussion

The commercial heat-sealing coatings tested provided heterogeneous barrier performance. However, SA-H showed properties similar to those of UC because of the diffused cracks in the surface, as shown in Figure 9e, that allow water, water vapor, and grease to be easily absorbed by the underneath fibers. Experimental formulations are able to achieve high barrier properties against both moisture and grease, even compared to commercial barrier dispersions, as already described in a previous study [7].

As a general statement, and considering the extent of the evaluated coatings, barrier and heat-sealing properties proved to be somehow inversely proportional, as shown in Figures 2, 4 and 5 and Table 5. In other words, grades that showed higher barrier performance generally did not heat-seal at low temperature, time, and pressure values. This can be explained by the latex softness, i.e., low glass transition temperature of the polymer, as shown in Table 4.

Previous studies discussed how cross-linking was positively associated with barrier properties and low sticking degrees [42,43]. Cross-linking, however, can also explain the tendency of the experimental formulations to fold cracking since a lower degree improves the elongation at break of the coatings [39]. Despite being highly cross-linked, the latex of experimental formulations showed an equivalent fold-cracked area that was of limited extent, highlighting a good balance between its low T_g and cross-linking, i.e., between stiffness and elongation at break.

Heat sealing was here described by means of average peel force and seal energy. Such parameters seemed to agree on sealing levels based on their values, i.e., a strong bond is formed at >2.5–3 N and >80–90 mJ, respectively, though it must be highlighted how such values correspond to a delamination of the paper substrate. This means that they are not representative of the coat-coat bond strength, which is of a higher magnitude. Despite its coat morphology, SA-H heat-seal ability was intact.

Kaolin proved a good admixture to modulate the heat-seal ability of the coated surfaces, requiring higher sealing temperatures to achieve cohesive adhesion between the two coated surfaces. By achieving good results at a sealing temperature of 80 °C or lower, experimental grades filled with low kaolin content (H39K 80) may be of interest for thermo-sensitive contents. Moreover, samples generally did not show blocking. Blocking and heat-sealing differed in test time (24 h vs. ≤2 s, respectively) and pressure (~0.003 MPa vs. ≤0.6 MPa, respectively). Despite being pressure the predominant factor among the two, the authors did not find the effect of pressure to be significant on the Pareto chart. However, this supports the idea that considering a wider range of pressures might turn it into a statistically significant factor. At an industrial level, the tension at which the paper is reeled, or the weight stacked above the sheets, should be minimized to reduce blocking occurrence; however, consistent with a report by Lyons and Reed [8], the addition of mineral fillers reduced the heat-seal ability of the experimental formulations. Indeed, a higher mineral content can reduce the equivalent area of latex on the surface of the coated paper, minimizing overall sticking to stacked or reeled substrates. Moreover, the difference in the standardized effect of the factors suggests that the experimental formulations could play a relevant role in reducing the energy consumption in a sealing line while carefully considering the optimization of the process in terms of a trade-off between productivity and sealing.

In this contribution, the authors propose a new method to measure crack folding, which is considered to be a simpler approach to those already present in the literature [22,39,44–46]. Indeed, it involves the folding of the sample followed by ink application, which in principle is absorbed by the underneath cellulose fibers only if cracks were formed during the folding. Therefore, the extent of the ink stain (obtained by image filtering and processing) is a quick yet semi-quantitative method to evaluate the presence, shape, and size of the crack formation. This methodology, however, seemed to be adequate only for coatings that provide a sufficient water barrier. Moreover, the proposed methodology is sensitive to the amount of ink applied to the sample and to the time interval between application and wiping. In principle, if more time is given and higher ink quantities are applied to the surface, the resulting stains may be greater. Good operator dexterity, or at least partial method automation, is required to further improve reliability and comparison across different research studies.

Nevertheless, the method was sufficiently accurate to clearly highlight the role of fold direction and coating orientation. The anisotropy of the substrate affected crack formation severity. The different behavior can be attributed to the bending stiffness along the fold line, which depends on both substrate thickness and fiber orientation, as supported by previous literature [19,20,30]. Instead, when referring to the coat orientation, being outside means that the coating is subjected to tensile stresses; on the contrary, if placed on the inside, the stress may be generally regarded as compression [19]. Given the reduction in the crack area with the folding line is parallel to MD, and on a much more important

reduction in crack area when the coat is placed on the inside rather than on the outside (Figure 7), a brittle behavior of the coating may be pointed out.

As the considered coatings are intended for food packaging applications, they will likely be positioned on the inside of the package itself, both for barrier and sealing properties, reducing the risk of crack formation. This is especially true to maintain the barrier properties guaranteed by the protective coating, which is of particular interest for some experimental formulations here considered, which can provide both barrier and sealing properties, as shown for A-H.

Additionally, increasing the pigment content led to crack formation. This is reasonable due to the intrinsic flexibility of the polymeric latex, which is greater than that of the pigment-loaded one. Such a system should perform like a polymeric matrix composite, in which increasing filler contents reduce the matrix (latex) continuity and, hence, the strain at break [44]. Therefore, higher kaolin contents are detrimental to fold cracking resistance [21]. Despite such behavior, the choice of a soft latex played a critical role in maintaining limited crack formation [8], achieving improved results compared to commercial solutions.

Finally, although higher kaolin content has been proven to be beneficial for water vapor and grease barrier properties [7], its content requires higher sealing times so that the polymeric chains can increase the interdiffusion degree, making up for a lower specific sealing surface. Similarly, crack formation is also negatively affected by pigment content; however, the low T_g of latex (close to 0 °C) counterweighted this effect. When developing a new formulation, processing properties should be taken into consideration alongside barrier properties from the outset, as a material that is not easy to process would be of scarce industrial interest.

5. Conclusions

The effect of kaolin content on processing and barrier properties was successfully evaluated. The amount of pigment inside waterborne dispersions proved to be a crucial factor modulating the minimum heat-seal ability in the investigated range, i.e., requiring longer seal times and higher temperatures from ≤80 °C of unpigmented formulation to >140 °C of H39K 40. Pressure, on the other hand, was found to be statistically irrelevant to heat-sealing properties. The low glass transition temperature of the latex made it possible to minimize the effects of fold cracking, showing that equivalent crack areas were generally reduced by >50% compared to the average value of commercial grades, with the highest improvement being found for fold lines parallel to the machine direction. However, fold cracking strongly impacted the coatings with lower WVTR, increasing H39K 40 WVTR by twofold. Nevertheless, the properties discussed in this study, combined with the excellent barrier properties of coatings with intermediate kaolin content, make them particularly appealing for industrial applications.

Author Contributions: Conceptualization, A.M.; methodology, A.M. and M.P. (Mauro Profaizer); investigation, A.M.; data curation, A.M.; writing—original draft preparation, A.M., M.P. (Mauro Profaizer) and M.V.D.; writing—review and editing, A.M., M.P. (Mauro Profaizer) and M.V.D.; visualization, A.M. and M.V.D.; supervision, M.P. (MariaPia Pedeferri) and B.D.C. All authors have read and agreed to the published version of the manuscript.

Funding: This research received no external funding.

Institutional Review Board Statement: Not applicable.

Informed Consent Statement: Not applicable.

Data Availability Statement: Data available on request. The data presented in this study are available on request from the corresponding author. Most data are contained within the article.

Conflicts of Interest: The authors declare no conflict of interest.

Appendix A

The heat-sealer can be observed in Figure A1. The pneumatic system comprises:

- An air regulator with operating pressure ranging 0–1 MPa;
- 5/2-way pneumatic valve featuring a manual knob to deviate the pressure;
- MAL double action pneumatic cylinder, characterized by a diameter of 16 mm and bore of 25 mm;
- Aluminum flat sealing tool.

Regarding the electronics and heating circuit, the hardware is composed of:

- Arduino Nano v3.0
- 12 V/40 W heating cartridge
- NTC 3950 100K thermistor
- 5 V Channel Relay Module Shield, capable to hold 10 A and 230 V (AC) or 30 V (DC)
- 12 V, 5 A power supply

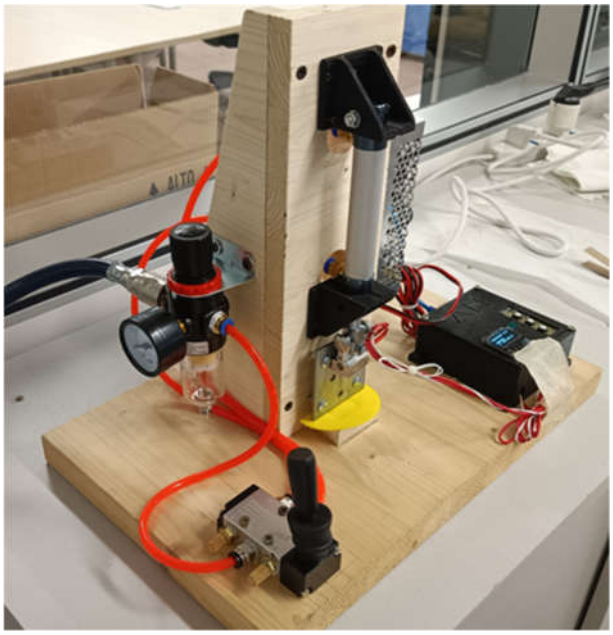

Figure A1. Picture of the heat-sealer used in this contribution.

The representative schematics of both the pneumatic and electronic circuit are represented in Figures A2 and A3, respectively.

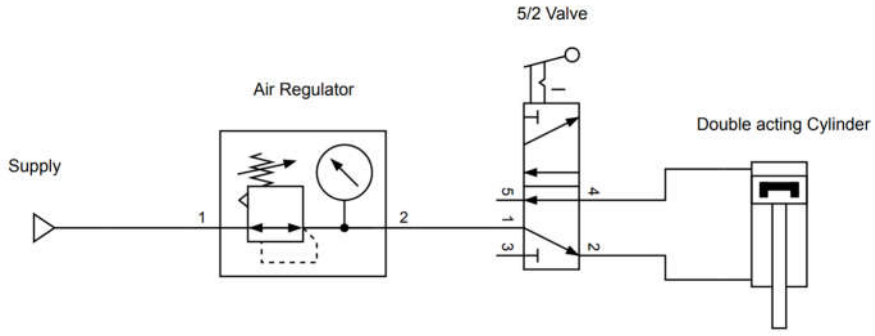

Figure A2. Schematic representing the pneumatic circuit of the heat-sealer.

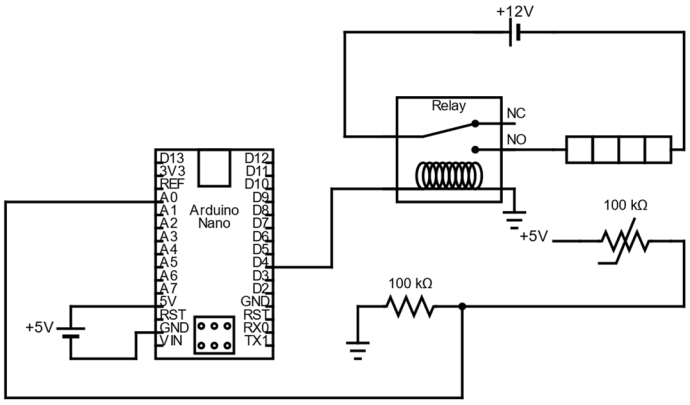

Figure A3. Schematic representing the main electric circuit of the heat-sealer (the display and buttons, which are visible in the bottom right corner of Figure A1, are not represented here to keep the schematic clear).

References

1. Marinelli, A.; Sossini, L.; Santi, R.; Del Curto, B. *Imballaggio Cellulosico Con Proprietà Barriera: Stato Dell'arte e Innovazione Dei Materiali*, 1st ed.; Edizioni Dativo Srl: Milan, Italy, 2022; ISBN 9788894310931.
2. Brander, J.; Thorn, I. Surface Application of Paper Chemicals; Blackie Academic and Professional: London, UK, 1997; ISBN 978-0-7514-0370-1.
3. Keddie, J.L. Film formation of latex. *Mater. Sci. Eng. R Rep.* **1997**, *21*, 101–170. https://doi.org/10.1016/s0927-796x(97)00011-9.
4. Cepi Paper-Based Packaging Recyclability Guidelines. Available online: https://www.cepi.org/wp-content/uploads/2020/10/Cepi_recyclability-guidelines.pdf (accessed on 15 July 2020).
5. CPI Design for Recyclability Guidelines. Available online: https://thecpi.org.uk/library/PDF/Public/Publications/Guidance Documents/CPI_guidelines_2022-WEB.pdf (accessed on 3 October 2022).
6. Marinelli, A.; Santi, R.; Del Curto, B. *Linee Guida per La Facilitazione Delle Attività Di Riciclo Degli Imballaggi a Prevalenza Cellulosica*, 1st ed.;CONAI: Milan, Italy, 2020; ISBN 9788894270020.
7. Marinelli, A.; Diamanti, M.V.; Pedeferri, M.; Del Curto, B. Kaolin-Filled Styrene-Butadiene-Based Dispersion Coatings for Paper-Based Packaging: Effect on Water, Moisture, and Grease Barrier Properties. *Coatings* **2023**, *13*, 195. https://doi.org/10.3390/coatings13010195.
8. Lyons, A.V.; Reed, G. Pigmented aqueous barrier coatings. *TAPPI J.* **2020**, *19*, 551–558. https://doi.org/10.32964/tj19.11.551.
9. Rissa, K.; Vähä-Nissi, M.; Lepistö, T.; Savolainen, A. Talc-Filled Water-Based Barrier Coatings. *Pap. Timber* **2002**, *84*, 1–6.
10. Schuman, T.; Karlsson, A.; Larsson, J.; Wikström, M.; Rigdahl, M. Characteristics of pigment-filled polymer coatings on paperboard. *Prog. Org. Coatings* **2005**, *54*, 360–371. https://doi.org/10.1016/j.porgcoat.2005.06.017.
11. Bollström, R.; Nyqvist, R.; Preston, J.; Salminen, P.; Toivakka, M. Barrier properties created by dispersion coating. *TAPPI J.* **2013**, *12*, 45–51. https://doi.org/10.32964/tj12.4.45.
12. Kugge, C.; Johnson, B. Improved barrier properties of double dispersion coated liner. *Prog. Org. Coatings* **2008**, *62*, 430–435. https://doi.org/10.1016/j.porgcoat.2008.03.006.
13. Zou, Y.; Hsieh, J.S.; Mehnert, E.; Kokoszka, J. The effect of pigments and latices on the properties of coated paper. *Colloids Surfaces A: Physicochem. Eng. Asp.* **2007**, *294*, 40–45. https://doi.org/10.1016/j.colsurfa.2006.07.046.
14. Niini, A.; Leminin, V.; Tanninen, P.; Varis, J.; Laukala, T. The durability of press-formed paperboard trays—Effects of sealing and drying. *Bioresources* **2012**, *16*, 236–248. https://doi.org/10.15376/biores.16.1.236-248.
15. Merabtene, M.; Tanninen, P.; Varis, J.; Leminen, V. Heat sealing evaluation and runnability issues of flexible paper materials in a vertical form fill seal packaging machine. *Bioresources* **2022**, *17*, 223–242. https://doi.org/10.15376/biores.17.1.223-242.
16. Hauptmann, M.; Bär, W.; Schmidtchen, L.; Bunk, N.; Abegglen, D.; Vishtal, A.; Wyser, Y. The sealing behavior of new monopolyolefin and paper-based film laminates in the context of bag form-fill-seal machines. *Packag. Technol. Sci.* **2021**, *34*, 117–126. https://doi.org/10.1002/pts.2544.
17. Andersson, C.; Ernstsson, M.; Järnström, L. Barrier properties and heat sealability/failure mechanisms of dispersion-coated paperboard. *Packag. Technol. Sci.* **2002**, *15*, 209–224. https://doi.org/10.1002/pts.590.
18. Kimpimäki, T.; Savolainen, A.V. *Barrier Dispersion Coating of Paper and Board. In Surface Application of Paper Chemicals*; Brander, J., Thron, I., Eds.; Springer: Dordrecht, The Netherlands, 1997; pp. 208–228; ISBN-978-94-010-7151-2.
19. Barbier, C.; Larsson, P.-L.; Östlund, S. Numerical investigation of folding of coated papers. *Compos. Struct.* **2005**, *67*, 383–394. https://doi.org/10.1016/j.compstruct.2004.01.024.
20. Kim, C.-K.; Lim, W.-S.; Lee, Y.K. Studies on the fold-ability of coated paperboard (I): Influence of latex on fold-ability during creasing/folding coated paperboard. *J. Ind. Eng. Chem.* **2010**, *16*, 842–847. https://doi.org/10.1016/j.jiec.2010.05.001.

21. Vähä-Nissi, M.; Savolainen, A. Filled Barrier Dispersion Coatings. In Proceedings of the Coating Conference Proceedings; TAPPI Press, Peachtree Corners, GA, USA, 1999.
22. Oh, K.; Sim, K.; Bin Jeong, Y.; Youn, H.J.; Lee, H.L.; Lee, Y.M.; Yeu, S.U. Effect of coating binder on fold cracking of coated paper. *Nord. Pulp Pap. Res. J.* **2015**, *30*, 361–368. https://doi.org/10.3183/npprj-2015-30-02-p361-368.
23. Alam, P.; Toivakka, M.; Carlsson, R.; Salminen, P.; Sandås, S. Balancing between Fold-crack Resistance and Stiffness. *J. Compos. Mater.* **2009**, *43*, 1265–1283. https://doi.org/10.1177/0021998308104227.
24. Barbier, C.; Larsson, P.-L.; Östlund, S. On the effect of high anisotropy at folding of coated papers. *Compos. Struct.* **2006**, *72*, 330–338. https://doi.org/10.1016/j.compstruct.2005.01.003.
25. Licciardello, F. Packaging, blessing in disguise. Review on its diverse contribution to food sustainability. *Trends Food Sci. Technol.* **2017**, *65*, 32–39. https://doi.org/10.1016/j.tifs.2017.05.003.
26. BS EN ISO 535:2014. Paper and Board. Determination of Water Absorptiveness. Cobb Method. Available online: https://bsol.bsigroup.com/Bibliographic/BibliographicInfoData/000000000030259603 (accessed on 5 January 2021).
27. BS ISO 2528:2017. Sheet Materials. Determination of Water Vapour Transmission Rate (WVTR). Gravimetric (Dish) Method Available online: https://bsol.bsigroup.com/Bibliographic/BibliographicInfoData/000000000030349864 (accessed on 3 March 2022).
28. BS ISO 16532-1:2008. Paper and Board. Determination of Grease Resistance. Permeability Test. Available online: https://bsol.bsigroup.com/Bibliographic/BibliographicInfoData/000000000030164327 (accessed on 2 February 2022).
29. BS EN 12702:2000. Adhesives for Paper and Board, Packaging and Disposable Sanitary Products. Determination of Blocking Behaviour of Potentially Adhesive Layers. Available online: https://bsol.bsigroup.com/Bibliographic/BibliographicInfoData/000000000030019633 (accessed on 15 November 2022).
30. Breskvar, K.; Ahtik, J.; Možina, K. CRACKING PHENOMENA OF COATINGS ON LABEL PAPERS. *Cellul. Chem. Technol.* **2021**, *55*, 289–297. https://doi.org/10.35812/cellulosechemtechnol.2021.55.29.
31. Bakker, S.; Bosveld, L.; Metselaar, G.A.; Esteves, A.C.C.; Schenning, A.P.H.J. Understanding and Improving the Oil and Water Barrier Performance of a Waterborne Coating on Paperboard. *ACS Appl. Polym. Mater.* **2022**, *4*, 6148–6155. https://doi.org/10.1021/acsapm.2c00937.
32. Al-Gharrawi, M.; Ollier, R.; Wang, J.; Bousfield, D.W. The influence of barrier pigments in waterborne barrier coatings on cellulose nanofiber layers. *J. Coatings Technol. Res.* **2021**, *19*, 3–14. https://doi.org/10.1007/s11998-021-00482-0.
33. Ying, H.; Qi, L.; Malotky, D.; Harris, J.; Kainz, B.; Drumright, R.; Liechty, W.; Mason, J. Coatings for sustainable paper-based flexible packaging: Barrier properties and processability. *TAPPI J.* **2022**, *28*, 617–622. https://doi.org/10.32964/tj21.11.617.
34. Bamps, B.; Guimaraes, R.M.M.; Duijsters, G.; Hermans, D.; Vanminsel, J.; Vervoort, E.; Buntinx, M.; Peeters, R. Characterizing Mechanical, Heat Seal, and Gas Barrier Performance of Biodegradable Films to Determine Food Packaging Applications. *Polymers* **2022**, *14*, 2569. https://doi.org/10.3390/polym14132569.
35. Ilhan, I.; Klooster, R.; Gibson, I. Effects of process parameters and solid particle contaminants on the seal strength of low-density polyethylene-based flexible food packaging films. *Packag. Technol. Sci.* **2021**, *34*, 413–421. https://doi.org/10.1002/pts.2567.
36. Michot, A.; Smith, D.S.; Degot, S.; Gault, C. Thermal conductivity and specific heat of kaolinite: Evolution with thermal treatment. *J. Eur. Ceram. Soc.* **2008**, *28*, 2639–2644. https://doi.org/10.1016/j.jeurceramsoc.2008.04.007.
37. Guo, Z.; Fan, Y. Heat seal properties of polymer–aluminum–polymer composite films for application in pouch lithium-ion battery. *RSC Adv.* **2016**, *6*, 8971–8979. https://doi.org/10.1039/C5RA27097A.
38. Leminen, V.; Mäkelä, P.; Tanninen, P.; Varis, J. Leakproof Heat Sealing of Paperboard Trays - Effect of Sealing Pressure and Crease Geometry. *Bioresources* **2015**, *10*, 6906–6915. https://doi.org/10.15376/biores.10.4.6906-6916.
39. Oh, K.; Seo, D.; Youn, H.J.; Lee, Y.M.; Yeu, S.U.; Lee, H.L. Effects of coating composition and folding direction on the fold cracking of coated paper. *Nord. Pulp Pap. Res. J.* **2016**, *31*, 347–353. https://doi.org/10.3183/npprj-2016-31-02-p347-353.
40. Wang, Q.; Ding, N. Coating factors influencing the fold cracking of coated papers. *Nord. Pulp Pap. Res. J.* **2020**, *35*, 419–431. https://doi.org/10.1515/npprj-2019-0051/MACHINEREADABLECITATION/RIS.
41. Zhu, Y.; Bousfield, D.; Gramlich, W.M. The influence of pigment type and loading on water vapor barrier properties of paper coatings before and after folding. *Prog. Org. Coatings* **2019**, *132*, 201–210. https://doi.org/10.1016/j.porgcoat.2019.03.031.
42. Schuman, T.; Wikström, M.; Rigdahl, M. Dispersion coating with carboxylated and cross-linked styrene–butadiene latices. 1. Effect of some polymer characteristics on film properties. *Prog. Org. Coatings* **2004**, *51*, 220–227. https://doi.org/10.1016/j.porgcoat.2004.07.015.
43. Gay, C.; Leibler, L. On Stickieness. *Phys. Today* **1999**, *52*, 48–52. https://doi.org/10.1063/1.882884.
44. Hashemi Najafi, S.M.; Bousfield, D.W.; Tajvidi, M. Cracking at the fold in double layer coated paper: the influence of latex and starch composition. *TAPPI J.* **2019**, *18*, 93–99. https://doi.org/10.32964/tj18.2.93.
45. Youn, H.J.; Sim, K.; Oh, K.D.; Lee, H.L.; Han, C.S.; Yeu, S.U.; Lee, Y.M. Fold cracking of coated paper: The effect of pulp fiber composition and beating. *Nord. Pulp Pap. Res. J.* **2012**, *27*, 445– 450. https://doi.org/10.3183/npprj-2012-27-02-p445-450.
46. Yang, A.; Xie, Y.; Renjung, W. From Theory to Practice: Improving the Foldcrack Resistance of Industrially Produced Triple Coated Paper. In Proceedings of the Papercon 2011, Covington, KY, USA, 1–4 May *2011*; pp. 1845–1858.